Automatica 137 (2022) 110024

Contents lists available at ScienceDirect

Automatica

journal homepage: www.elsevier.com/locate/automatica

Brief paper

Robust adaptive learning for attitude control of rigid bodies with initial alignment errors[☆]

Fan Zhang [a,b], Deyuan Meng [a,b,*], Xuefang Li [c]

[a] The Seventh Research Division, Beihang University (BUAA), Beijing 100191, PR China
[b] School of Automation Science and Electrical Engineering, Beihang University (BUAA), Beijing 100191, PR China
[c] School of Intelligent Systems Engineering, Sun Yat-Sen University, Guangzhou 510275, PR China

ARTICLE INFO

Article history:
Received 15 January 2021
Received in revised form 25 May 2021
Accepted 18 September 2021
Available online 24 November 2021

Keywords:
Adaptive iterative learning control
Attitude tracking control
Deadzone mechanism
Initial alignment error
Rigid body

ABSTRACT

In the attitude tracking control tasks of rigid-body systems, initial alignment errors are recognized as one of the main factors that hinder the effective controller design and thus the control accuracy improvement. To overcome this difficulty, we develop a novel adaptive iterative learning control (ILC) scheme to achieve the attitude tracking control tasks with high precision for rigid bodies. Owing to the newly employed deadzone mechanism in the parametric updating law, the proposed adaptive ILC scheme is able to deal with initial alignment errors properly without imposing extra requirements to the system dynamics. Moreover, by utilizing the quaternion-based description in the system dynamics, various uncertainties, including external iteration-varying disturbances and unknown system parameters, can be addressed together by a single scalar estimation scheme. The convergence of the proposed adaptive ILC scheme is analyzed rigorously with a Lyapunov-like theory by virtue of newly introducing a modified composite energy function. In addition, to demonstrate its effectiveness, the proposed adaptive ILC method is applied to the attitude tracking of a spacecraft, which shows excellent control performances despite various uncertainties.

1. Introduction

Rigid bodies and their attitude control techniques play an important role in many real-time applications (Chaturvedi et al., 2011), such as spacecraft (Zou et al., 2020), robots (Sutyasadi & Parnichun, 2015), and aerial vehicles (He et al., 2019). In literature, in order to ensure the robust stability and/or tracking performance of rigid bodies, various effective control approaches have been developed, such as PD-based control (Wen & Kreutz-Delgado, 1991), adaptive control (Ahmed et al., 1998), optimal control (Luo et al., 2005), and variable structure control (Hu et al., 2013). Of note is that the aforementioned works mainly focus on the steady-state responses of the rigid bodies. In practice, especially for remote sensing and observation missions, the transient performance of attitude tracking, however, is also critically important, such that the rigid spacecraft exactly tracks the predefined attitude trajectory over a period from the very beginning to the end, since the exactly identical viewing condition is required to observe the change in the specific area (Wu et al., 2015). In such a case, it might be difficult to achieve accurate tracking tasks by applying conventional feedback control techniques, especially for systems with the existence of initial alignment errors.

As an intelligent control approach, iterative learning control (ILC) aims at perfect tracking performance at each time instant instead of asymptotic convergence along the time axis (Bristow et al., 2006; Lee & Lee, 2007). Under the framework of ILC, the transient control performance of the controlled system can be improved gradually by learning from the past control experience. In the past years, ILC has made great progresses in the underlying theory (Ahn et al., 2007; Chien & Tayebi, 2008; French & Rogers, 2000; Xu, 2011; Xu & Tan, 2002; Yu & Li, 2017; Yu et al., 2013), and has been applied in many fields (Chen et al., 2019; Dai et al., 2018; He et al., 2018) due to its simplicity in implementation. However, it is well-known that to achieve an accurate/perfect tracking performance, the strict repetitiveness of system dynamics, such as identical initial state, identical system dynamics, etc., is indispensable (Ahn et al., 2007; Xu, 2011), which might be unachievable in practice. For instance, initial alignment errors and iteration-varying system uncertainties usually exist in attitude control of rigid bodies. In ILC field, many

☆ This work was supported by the National Natural Science Foundation of China under Grant 61873013, Grant 61922007 and Grant 62003376. The material in this paper was not presented at any conference. This paper was recommended for publication in revised form by Associate Editor Peng Shi under the direction of Editor Thomas Parisini.

* Corresponding author at: The Seventh Research Division, Beihang University (BUAA), Beijing 100191, PR China.

E-mail addresses: zhangfan_buaa@buaa.edu.cn (F. Zhang), dymeng@buaa.edu.cn (D. Meng), lixuef25@mail.sysu.edu.cn (X. Li).

https://doi.org/10.1016/j.automatica.2021.110024
0005-1098/

efforts have been devoted to handling the iteration-varying uncertainties under both the frameworks of contraction-mapping-based ILC and composite-energy-function (CEF)-based ILC (Chien & Tayebi, 2008; French & Rogers, 2000; Xu & Tan, 2002; Yu & Li, 2017; Yu et al., 2013). Nonetheless, for ILC with non-identical initial states, how to design the controller and analyze the convergence correspondingly is still a challenging issue, especially under the framework of CEF-based adaptive ILC, which relies on the estimated parameters from the previous iteration.

In the past years, to remove/relax the identical initial condition (i.i.c.), some progresses have already been made (Chien, 2008; Jin, 2017; Meng, 2019; Meng & Moore, 2017; Meng & Zhang, 2018; Sun & Wang, 2002; Xie & Sun, 2009; Xu & Yan, 2005). However, most of these works are conducted under the framework of contraction mapping methodology. For the scenarios of adaptive ILC with non-identical initial states, there are only a few investigations. For example, a robust adaptive ILC with a rectifying action (Sun & Wang, 2002) on the initial state is developed in Jin (2017), where the rectifying action is employed over a small time interval in each iteration. Due to the limitations in hardware, it is hard to rectify initial alignment errors when they are sufficiently small. Moreover, for a class of high order strict-feedback nonlinear systems with initial alignment errors, a time-varying boundary layer is utilized to construct a fuzzy adaptive ILC scheme (Chien, 2008). Additionally, a finite-time boundary layer-based ILC has been introduced in Xie and Sun (2009) to deal with initial alignment errors. Nevertheless, it is difficult to apply the aforementioned methods directly to the attitude tracking control system with three degree-of-freedom since the derivative of the boundary layer function only exists for the system with one degree-of-freedom.

Motivated by the above observations, a novel adaptive ILC scheme is proposed to address the attitude tracking control problem for rigid bodies with initial alignment errors as well as system uncertainties. By virtue of a newly designed parametric updating law equipped with a deadzone mechanism, initial alignment errors can be treated efficiently, and the convergence of the tracking errors can be guaranteed. In contrast to existing works, the main contributions of the present work can be summarized as follows.

(1) A novel adaptive ILC scheme is proposed in the present work, which is able to effectively handle the system model uncertainties, iteration-varying external disturbances as well as initial alignment errors. In contrast to conventional CEF-based ILC (Chien & Tayebi, 2008; French & Rogers, 2000; Tayebi, 2004), this work newly provides a design and analysis framework for adaptive ILC to deal with various iteration-varying uncertainties, thereby expanding the application scope of adaptive ILC.
(2) Different from Meng (2019), Meng and Moore (2017), Meng and Zhang (2018) that aim at explicitly coping with contraction-mapping-based ILC with initial alignment errors, this work is targeted at adaptive ILC with initial alignment errors, which is analyzed under the framework of CEF methodology. To properly handle initial alignment errors, a newly designed deadzone mechanism is employed in the parametric updating law, which can prevent the accumulation of initial alignment errors of the system and ensure the uniform convergence of the tracking errors.
(3) The proposed scheme is applied to the attitude tracking control of rigid-body systems, which shows an impressive tracking performance. By taking advantage of the quaternion-based representation of the system model, various system uncertainties, such as the unknown system parameters and the iteration-varying external disturbances, can be treated together by introducing a single scalar parametric estimating law. This does not only simplify the controller design process but also would make the controller more convenient to be implemented in practice by contrast with, e.g., Chien and Tayebi (2008), Tayebi (2004), Wu et al. (2015).

The rest of this paper is organized as follows. In Section 2, some preliminary knowledge of the quaternion-based system representation is introduced to facilitate the subsequent controller design. In Section 3, the problem formulation for the attitude tracking of rigid bodies is presented, followed by the adaptive ILC design and convergence analysis in Section 4. Case studies and conclusions are provided in Sections 5 and 6 , respectively.

Notations. Let $\mathbb{Z}_+ = \{0, 1, 2, \ldots\}$ be the set of nonnegative integers, and $\boldsymbol{I}_3 \in \mathbb{R}^{3\times 3}$ be the identity matrix. For any $\boldsymbol{A} = [a_{ij}] \in \mathbb{R}^{m\times n}$, $\|\boldsymbol{A}\|$ denotes the spectral norm of $\boldsymbol{A}$, and $\|\boldsymbol{A}\|_\infty$ denotes the maximum row sum norm of $\boldsymbol{A}$. For any positive definite matrix $\boldsymbol{B} = [b_{ij}] \in \mathbb{R}^{m\times m}$, $\lambda_{\min}(\boldsymbol{B})$ and $\lambda_{\max}(\boldsymbol{B})$ denote the minimal and maximal eigenvalues of $\boldsymbol{B}$, respectively. For any $\boldsymbol{x} = [x_1, x_2, x_3]^{\mathrm{T}} \in \mathbb{R}^3$, the sign operator and the vector cross-product operator are, respectively, defined as

$$\operatorname{sgn}(\boldsymbol{x}) = \begin{bmatrix} \operatorname{sgn}(x_1) \\ \operatorname{sgn}(x_2) \\ \operatorname{sgn}(x_3) \end{bmatrix} \quad \text{and} \quad \boldsymbol{x}^\times = \begin{bmatrix} 0 & -x_3 & x_2 \\ x_3 & 0 & -x_1 \\ -x_2 & x_1 & 0 \end{bmatrix}.$$

According to the above definitions, the following operations hold for any $\boldsymbol{x}, \boldsymbol{y} \in \mathbb{R}^3$:

$$\left(\boldsymbol{x}^\times\right)^{\mathrm{T}} = -\boldsymbol{x}^\times, \qquad \boldsymbol{x}^\times \boldsymbol{y} = -\boldsymbol{y}^\times \boldsymbol{x}, \qquad \boldsymbol{x}^{\mathrm{T}} \boldsymbol{x}^\times = \boldsymbol{0},$$
$$(\boldsymbol{x}+\boldsymbol{y})^\times = \boldsymbol{x}^\times + \boldsymbol{y}^\times, \qquad \left\|\boldsymbol{x}^\times\right\| = \|\boldsymbol{x}\|,$$

where $\boldsymbol{0}$ is the trivial zero vector.

2. Preliminaries

In this section, some useful concepts and notations of the unit quaternion representation are first introduced. Then the quaternion-based attitude dynamics and kinematics for a rigid body is presented to facilitate the controller design and convergence analysis that is developed in the subsequent sections.

In practical applications, the quaternion representation is developed based on Euler's rotation theorem, which states that the relative orientation of the body-fixed frame $\mathcal{F}_B$ $(O - X_B Y_B Z_B)$ with respect to the inertial frame $\mathcal{F}_I$ $(O - X_I Y_I Z_I)$ can be presented as only one rotation about a fixed axis (Chou, 1992). The quaternion is usually treated as a four-parameter set, denoted by $(\varepsilon, \boldsymbol{q})$, where $\varepsilon \in \mathbb{R}$ and $\boldsymbol{q} \in \mathbb{R}^3$ denote the scalar part and vector part of the quaternion, respectively. In detail, according to Section 2.2 in Hughes (2004), the quaternion $(\varepsilon, \boldsymbol{q})$ is represented as $\varepsilon = \cos(\varphi/2)$ and $\boldsymbol{q} = \boldsymbol{e}\sin(\varphi/2)$, where the unit vector $\boldsymbol{e} \in \mathbb{R}^3$ is the Euler axis and $\varphi \in \mathbb{R}$ is the Euler angle. It is obvious that the quaternion satisfies $\varepsilon^2 + \boldsymbol{q}^{\mathrm{T}}\boldsymbol{q} = 1$.

According to the above definitions, the attitude dynamics and kinematics of a rigid body can be represented in the framework of the quaternion as follows (see also Wen and Kreutz-Delgado (1991) for the detailed derivations):

$$\begin{aligned} \boldsymbol{J}\dot{\boldsymbol{\omega}}_k(t) &= -\boldsymbol{\omega}_k^\times(t)\boldsymbol{J}\boldsymbol{\omega}_k(t) + \boldsymbol{u}_k(t) + \boldsymbol{d}_k(t) \\ \dot{\boldsymbol{q}}_k(t) &= \frac{1}{2}\left[\boldsymbol{q}_k^\times(t) + \varepsilon_k(t)\boldsymbol{I}_3\right]\boldsymbol{\omega}_k(t) \\ \dot{\varepsilon}_k(t) &= -\frac{1}{2}\boldsymbol{q}_k^{\mathrm{T}}(t)\boldsymbol{\omega}_k(t), \end{aligned} \tag{1}$$

where $k \in \mathbb{Z}_+$ denotes the iteration index to indicate that the rigid body performs a repetitive mission; $t \in [0, T]$ is the operation time; $\boldsymbol{\omega}_k(t) \in \mathbb{R}^3$ denotes the angular velocity of the rigid body with respect to the inertial frame $\mathcal{F}_I$, which is expressed in the body-fixed frame $\mathcal{F}_B$; $\boldsymbol{J} \in \mathbb{R}^{3\times 3}$ denotes the inertia matrix

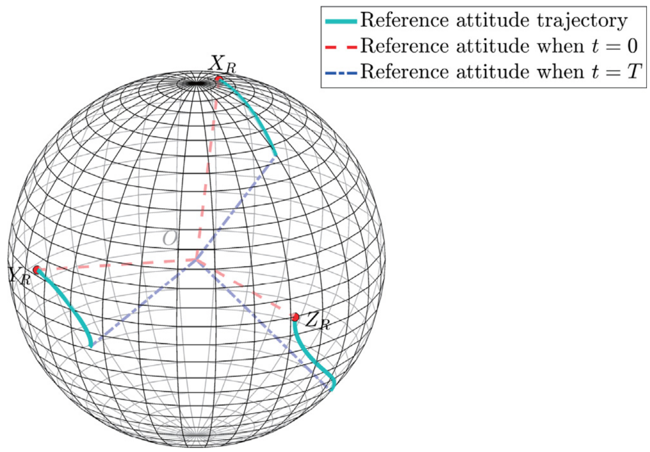

Fig. 1. Reference attitude trajectory with three degree-of-freedom on attitude sphere. Red dot: the starting point.

that is bounded and positive definite; and $\boldsymbol{u}_k(t) \in \mathbb{R}^3$ and $\boldsymbol{d}_k(t) \in \mathbb{R}^3$ are the control torque and external disturbance, respectively. Furthermore, let $\boldsymbol{J} = k_J \boldsymbol{J}_n$ with $k_J > 0$ being some unknown constant and $\boldsymbol{J}_n$ being the nominal inertia matrix, and $\boldsymbol{d}_k(t)$ be uniformly bounded along the iteration axis, i.e, $\sup_{k\in\mathbb{Z}_+} \|\boldsymbol{d}_k(t)\| \le \beta_d(t)$, where $\beta_d(t) > 0$ denotes some finite (unknown) bound.

3. Problem statement

In this section, we firstly present the reference attitude trajectory and the attitude tracking error dynamics and kinematics, which are followed by the attitude tracking problem formulation.

3.1. Reference attitude trajectory and error dynamics

Let $\boldsymbol{q}_d(t) \in \mathbb{R}^3$ and $\boldsymbol{\omega}_d(t) \in \mathbb{R}^3$, $\forall t \in [0, T]$ represent the reference quaternion and the reference angular velocity of the reference frame $\mathcal{F}_R$ $(O-X_RY_RZ_R)$ with respect to the inertial frame $\mathcal{F}_I$, respectively, and satisfy the kinematics in (1). The corresponding reference attitude trajectory with three degree-of-freedom on the attitude sphere is illustrated in Fig. 1.

Moreover, let $(\delta\varepsilon_k(t), \delta\boldsymbol{q}_k(t)) \in \mathbb{R} \times \mathbb{R}^3$ and $\delta\boldsymbol{\omega}_k(t) \in \mathbb{R}^3$ be the quaternion error and the angular velocity error, respectively. Based on the quaternion multiplication rule and the rigid body kinematics presented in Sections 2.2 and 2.3 of Hughes (2004), we can obtain

$$\begin{bmatrix} \delta\varepsilon_k(t) \\ \delta\boldsymbol{q}_k(t) \end{bmatrix} = \begin{bmatrix} \varepsilon_d(t)\varepsilon_k(t) + \boldsymbol{q}_k^{\mathrm{T}}(t)\boldsymbol{q}_d(t) \\ \varepsilon_d(t)\boldsymbol{q}_k(t) - \varepsilon_k(t)\boldsymbol{q}_d(t) + \boldsymbol{q}_k^{\times}(t)\boldsymbol{q}_d(t) \end{bmatrix} \tag{2}$$

and

$$\delta\boldsymbol{\omega}_k(t) = \boldsymbol{\omega}_k(t) - \boldsymbol{R}_k(t)\boldsymbol{\omega}_d(t), \tag{3}$$

where $\boldsymbol{R}_k(t) \in SO(3)$ denotes the rotation matrix from $\mathcal{F}_R$ to $\mathcal{F}_B$ which is given by

$$\begin{aligned} \boldsymbol{R}_k(t) = {} & \left[\delta\varepsilon_k(t)\delta\varepsilon_k(t) - \delta\boldsymbol{q}_k^{\mathrm{T}}(t)\delta\boldsymbol{q}_k(t)\right]\boldsymbol{I}_3 + 2\delta\boldsymbol{q}_k(t)\delta\boldsymbol{q}_k^{\mathrm{T}}(t) \\ & - 2\delta\varepsilon_k(t)\delta\boldsymbol{q}_k^{\times}(t). \end{aligned} \tag{4}$$

Additionally, according to Section 2.3 in Hughes (2004), $\dot{\boldsymbol{R}}_k(t) = -\delta\boldsymbol{\omega}_k^{\times}(t)\boldsymbol{R}_k(t)$ holds. This, together with (1) and (3), implies the attitude tracking error system of a rigid body can be obtained as

$$\begin{aligned} \boldsymbol{J}\delta\dot{\boldsymbol{\omega}}_k(t) &= \boldsymbol{J}\left[\delta\boldsymbol{\omega}_k^{\times}(t)\boldsymbol{R}_k(t)\boldsymbol{\omega}_d(t) - \boldsymbol{R}_k(t)\dot{\boldsymbol{\omega}}_d(t)\right] \\ &\quad - \boldsymbol{\omega}_k^{\times}(t)\boldsymbol{J}\boldsymbol{\omega}_k(t) + \boldsymbol{u}_k(t) + \boldsymbol{d}_k(t) \\ \delta\dot{\boldsymbol{q}}_k(t) &= \frac{1}{2}\left[\delta\boldsymbol{q}_k^{\times}(t) + \delta\varepsilon_k(t)\boldsymbol{I}_3\right]\delta\boldsymbol{\omega}_k(t) \\ \delta\dot{\varepsilon}_k(t) &= -\frac{1}{2}\delta\boldsymbol{q}_k^{\mathrm{T}}(t)\delta\boldsymbol{\omega}_k(t), \end{aligned} \tag{5}$$

where $\dot{\boldsymbol{\omega}}_d(t)$ is the derivative of $\boldsymbol{\omega}_d(t)$. Generally, $\boldsymbol{\omega}_d(t)$ and $\dot{\boldsymbol{\omega}}_d(t)$ are supposed to be bounded for $t \in [0, T]$.

To facilitate the controller design and convergence analysis in the subsequent section, we have the following lemma that presents three useful properties of the system (5).

Lemma 1. *For the attitude tracking error system (5), the following statements hold.*

(1) $\left\|\delta\varepsilon_k(t)\boldsymbol{I}_3 - \delta\boldsymbol{q}_k^{\times}(t)\right\| = 1$ *and* $\left\|\delta\boldsymbol{q}_k(t)\right\| \le 1$.
(2) The rotation matrix $\boldsymbol{R}_k(t)$ *is orthogonal.*
(3) $[\boldsymbol{R}_k(t)\boldsymbol{\omega}_d(t)]^{\times}\boldsymbol{J} + \boldsymbol{J}[\boldsymbol{R}_k(t)\boldsymbol{\omega}_d(t)]^{\times}$ *is skew symmetric.*

Proof. See the Appendix.

3.2. Problem statement

Given the rigid-body system (1) performing a repetitive attitude tracking task, the objective of the present work is to develop an adaptive ILC scheme such that the high-precision attitude tracking performance can be achieved. To be specific, we are interested in realizing the following two objectives.

(1) The perfect tracking control performance is achievable in the iteration domain, i.e.,

$$\begin{cases} \lim_{k\to\infty} \left\|\delta\boldsymbol{q}_k(t)\right\| = 0 \\ \lim_{k\to\infty} \left\|\delta\boldsymbol{\omega}_k(t)\right\| = 0 \end{cases} \quad \forall t \in [0, T]\,, \tag{6}$$

if initial alignment errors are zero despite the unmodeled dynamics and external disturbances.

(2) The tracking errors converge gradually to a neighborhood of the origin as the iteration number increases in the presence of initial alignment errors, namely,

$$\begin{cases} \limsup_{k\to\infty} \left\|\delta\boldsymbol{q}_k(t)\right\| \le \beta_{\delta q_{\sup}} \\ \limsup_{k\to\infty} \left\|\delta\boldsymbol{\omega}_k(t)\right\| \le \beta_{\delta\omega_{\sup}} \end{cases} \quad \forall t \in [0, T]\,, \tag{7}$$

where $\beta_{\delta q_{\sup}} > 0$ and $\beta_{\delta\omega_{\sup}} > 0$ are two small constants depending continuously on initial alignment errors.

Moreover, for the considered rigid-body system (1), we have an assumption on initial alignment errors.

Assumption 2. Let initial alignment errors $\delta\boldsymbol{\omega}_k(0)$ and $\delta\boldsymbol{q}_k(0)$ be bounded, namely, there exist two positive constants $\beta_{\delta q0}$ and $\beta_{\delta\omega 0}$ such that $\left\|\delta\boldsymbol{q}_k(0)\right\| \le \beta_{\delta q0}$ and $\|\delta\boldsymbol{\omega}_k(0)\| \le \beta_{\delta\omega 0}$, $\forall k \in \mathbb{Z}_+$.

Remark 3. In ILC area, especially in the adaptive ILC field, i.i.c. is a common condition ensuring the perfect tracking performance (Tayebi, 2004). However, it may not hold in practical applications, and how to extend the adaptive ILC to systems with non-identical initial states is still challenging (Xu & Yan, 2005). As the main contributions of the present work, we will provide two convergent results for both the scenarios without and with i.i.c. It is worthy to note that to handle initial alignment errors, a novel adaptive ILC scheme and a modified CEF-based convergence analytical approach are proposed.

4. Controller design and convergence analysis

In this section, an adaptive learning controller together with a parametric updating law is developed for the attitude tracking control of the rigid-body system (1). In order to deal with initial alignment errors and ensure the convergence of the proposed control scheme, a modified CEF equipped with a deadzone mechanism is newly introduced, which greatly extends adaptive ILC to nonlinear systems with initial alignment errors.

To achieve the high-precision attitude tracking objective, the following adaptive learning controller is proposed for the attitude tracking error system (5):

$$\boldsymbol{u}_k(t) = -\boldsymbol{K}_d\delta\boldsymbol{\omega}_k(t) - \hat{\theta}_k(t)\,\mathrm{sgn}\,(\delta\boldsymbol{\omega}_k(t)), \tag{8}$$

where the matrix $\boldsymbol{K}_d \in \mathbb{R}^{3\times 3}$ is positive definite, and $\hat{\theta}_k(t) \in \mathbb{R}$ is used to estimate the system uncertainty $\theta(t) \in \mathbb{R}$ satisfying

$$\theta(t) \geq \|\boldsymbol{J}\| + \|\boldsymbol{J}\|\,\|\boldsymbol{\omega}_d(t)\|^2 + \|\boldsymbol{J}\|\,\|\dot{\boldsymbol{\omega}}_d(t)\| + \beta_d(t) \tag{9}$$

with $\beta_d(t)$ defined in Section 2. The updating law for $\hat{\theta}_k(t)$ is designed as

$$\begin{aligned}&\hat{\theta}_k(t) = \hat{\theta}_{k-1}(t) + \gamma\zeta_k(t)\delta\boldsymbol{\omega}_k^{\mathrm{T}}(t)\,\mathrm{sgn}(\delta\boldsymbol{\omega}_k(t))\\&\hat{\theta}_{-1}(t) = 0, \quad \forall t \in [0, T],\end{aligned} \tag{10}$$

where $\gamma > 0$ is the learning gain, and $\zeta_k(t)$ satisfies

$$\zeta_k(t) = \begin{cases} 1 - \dfrac{\beta_{dz}}{E_k(t)} & \text{if } E_k(t) > \beta_{dz} \\ 0 & \text{otherwise} \end{cases} \tag{11}$$

with β_{dz} and $E_k(t)$ defined as

$$\begin{aligned}\beta_{dz} &= \left[\lambda_{\max}(\boldsymbol{J}_n)\left(\beta_{\delta q0}^2 + \beta_{\delta\omega 0}^2\right)\right]^{\frac{1}{2}}\\ E_k(t) &= \left[\delta\boldsymbol{q}_k^{\mathrm{T}}(t)\boldsymbol{J}_n\delta\boldsymbol{q}_k(t) + \delta\boldsymbol{\omega}_k^{\mathrm{T}}(t)\boldsymbol{J}_n\delta\boldsymbol{\omega}_k(t)\right]^{\frac{1}{2}}.\end{aligned} \tag{12}$$

Remark 4. In the parametric updating law (11), $\zeta_k(t)$ is newly introduced to deal with initial alignment errors. By virtue of the deadzone property, a modified CEF will be developed to prevent the accumulation of initial alignment errors that may cause the divergence of the controller. The idea is novel in terms of both the controller design and the convergence analysis in adaptive ILC area, which would significantly widen the application scope of adaptive ILC.

The convergence property of the proposed adaptive ILC scheme is summarized in the following theorem.

Theorem 5. *For the attitude tracking error system (5) under Assumption 2, let the adaptive learning controller (8) and the parametric updating law (10) be applied. Then the robust tracking objective (7) can be achieved.*

In order to show the convergence property of the proposed controller, we develop the following modified CEF

$$W_k(t) = V_k(t) + \frac{1}{2}\int_0^t \gamma^{-1}\tilde{\theta}_k^2(\tau)\mathrm{d}\tau \tag{13}$$

with $\tilde{\theta}_k(t) \triangleq \theta(t) - \hat{\theta}_k(t)$ representing the estimation error and $V_k(t)$ defined as

$$V_k(t) = \iota_k(t)\left\{\left[V_{q,k}(t) + V_{\omega,k}(t)\right]^{\frac{1}{2}} - k_J^{\frac{1}{2}}\beta_{dz}\right\}^2 \tag{14}$$

where $V_{q,k}(t)$ and $V_{\omega,k}(t)$ are designed as

$$\begin{aligned}V_{q,k}(t) &\triangleq \frac{1}{2}\delta\boldsymbol{q}_k^{\mathrm{T}}(t)\boldsymbol{J}\delta\boldsymbol{q}_k(t)\\ V_{\omega,k}(t) &\triangleq \frac{1}{2}\delta\boldsymbol{\omega}_k^{\mathrm{T}}(t)\boldsymbol{J}\delta\boldsymbol{\omega}_k(t),\end{aligned}$$

and $\iota_k(t)$ is an indicator function described by

$$\iota_k(t) = \begin{cases} 1 & \text{if } \left[V_{q,k}(t) + V_{\omega,k}(t)\right]^{\frac{1}{2}} > k_J^{\frac{1}{2}}\beta_{dz} \\ 0 & \text{otherwise.}\end{cases} \tag{15}$$

Proof of Theorem 5. The analysis is divided into three parts. The first part shows the non-increasing property of the CEF, which is followed by the analysis of the boundedness for the CEF at the initial iteration. In the third part, the convergence of the tracking errors is presented.

Part (1): The non-increasing property of $W_k(t)$ along the iteration axis. According to the definition of $W_k(t)$ presented in (13), we can obtain that the difference between $W_k(t)$ and $W_{k-1}(t)$ can be calculated as

$$\Delta W_k(t) \triangleq W_k(t) - W_{k-1}(t) \tag{16}$$

Moreover, according to Assumption 2 and the definitions shown in (14) and (15), we can obtain

$$V_k(0) = 0, \tag{17}$$

which is critically important for the subsequent proof of non-positive property of $\Delta W_k(t)$ and implies that

$$\begin{aligned}\Delta W_k(t) = &\int_0^t \dot{V}_k(\tau)d\tau - V_{k-1}(t)\\ &- \frac{1}{2}\gamma^{-1}\int_0^t\left[2\bar{\theta}_k(\tau)\tilde{\theta}_k(\tau) + \bar{\theta}_k^2(\tau)\right]\mathrm{d}\tau,\end{aligned} \tag{18}$$

where $\bar{\theta}_k(t) \triangleq \hat{\theta}_k(t) - \hat{\theta}_{k-1}(t)$.

Let us first look into $\dot{V}_k(t)$ in the first term on the right hand side of (18). Considering (14)–(15), we have $\iota_k(t) = 1$ and

$$\begin{aligned}\dot{V}_k(t) &= \left\{1 - \frac{k_J^{\frac{1}{2}}\beta_{dz}}{\left[V_{q,k}(t) + V_{\omega,k}(t)\right]^{\frac{1}{2}}}\right\}\left[\dot{V}_{q,k}(t) + \dot{V}_{\omega,k}(t)\right]\\ &= \left[1 - \frac{\beta_{dz}}{E_k(t)}\right]\left[\dot{V}_{q,k}(t) + \dot{V}_{\omega,k}(t)\right]\end{aligned}$$

when $\left[V_{q,k}(t) + V_{\omega,k}(t)\right]^{\frac{1}{2}} > k_J^{\frac{1}{2}}\beta_{dz}$, while for the scenario with $\left[V_{q,k}(t) + V_{\omega,k}(t)\right]^{\frac{1}{2}} \leq k_J^{\frac{1}{2}}\beta_{dz}$, we have $\iota_k(t) = 0$ and $\dot{V}_k(t) = 0$. Consequently, the smoothness of $V_k(t)$ can be guaranteed and the expression of $\dot{V}_k(t)$ can be obtained as

$$\dot{V}_k(t) = \zeta_k(t)\left[\dot{V}_{q,k}(t) + \dot{V}_{\omega,k}(t)\right], \tag{19}$$

where $\zeta_k(t)$ has been defined in (11).

Moreover, by Lemma 1, it is not difficult to derive

$$\begin{aligned}\dot{V}_{q,k}(t) &= \delta\dot{\boldsymbol{q}}_k^{\mathrm{T}}(t)\boldsymbol{J}\delta\boldsymbol{q}_k(t)\\ &= \frac{1}{2}\delta\boldsymbol{\omega}_k^{\mathrm{T}}(t)\left[\delta\varepsilon_k(t)\boldsymbol{I}_3 - \delta\boldsymbol{q}_k^{\times}(t)\right]\boldsymbol{J}\delta\boldsymbol{q}_k(t)\\ &\leq \left\|\delta\boldsymbol{\omega}_k^{\mathrm{T}}(t)\right\|\,\|\boldsymbol{J}\|.\end{aligned} \tag{20}$$

Similarly, we can obtain

$$\dot{V}_{\omega,k}(t) = \delta\boldsymbol{\omega}_k^{\mathrm{T}}(t)\boldsymbol{J}\delta\dot{\boldsymbol{\omega}}_k(t), \tag{21}$$

which leads to

$$\begin{aligned}\dot{V}_{\omega,k}(t) = &\,\delta\boldsymbol{\omega}_k^{\mathrm{T}}(t)\boldsymbol{J}\left[\delta\boldsymbol{\omega}_k^{\times}(t)\boldsymbol{R}_k(t)\boldsymbol{\omega}_d(t) - \boldsymbol{R}_k(t)\dot{\boldsymbol{\omega}}_d(t)\right]\\ &- \delta\boldsymbol{\omega}_k^{\mathrm{T}}(t)\boldsymbol{\omega}_k^{\times}(t)\boldsymbol{J}\boldsymbol{\omega}_k(t) + \delta\boldsymbol{\omega}_k^{\mathrm{T}}(t)\boldsymbol{d}_k(t) + \delta\boldsymbol{\omega}_k^{\mathrm{T}}(t)\boldsymbol{u}_k(t).\end{aligned} \tag{22}$$

Moreover, one can reasonably obtain

$$\begin{aligned}&\delta\boldsymbol{\omega}_k^{\mathrm{T}}(t)\boldsymbol{J}\left[\delta\boldsymbol{\omega}_k^{\times}(t)\boldsymbol{R}_k(t)\boldsymbol{\omega}_d(t) - \boldsymbol{R}_k(t)\dot{\boldsymbol{\omega}}_d(t)\right]\\ =&-\delta\boldsymbol{\omega}_k^{\mathrm{T}}(t)\boldsymbol{J}\left[\boldsymbol{R}_k(t)\boldsymbol{\omega}_d(t)\right]^{\times}\delta\boldsymbol{\omega}_k(t) - \delta\boldsymbol{\omega}_k^{\mathrm{T}}(t)\boldsymbol{J}\boldsymbol{R}_k(t)\dot{\boldsymbol{\omega}}_d(t)\end{aligned} \tag{23}$$

as well as

$$\begin{aligned}&\delta\boldsymbol{\omega}_k^{\mathrm{T}}(t)\boldsymbol{\omega}_k^{\times}(t)\boldsymbol{J}\boldsymbol{\omega}_k(t)\\ =&\,\delta\boldsymbol{\omega}_k^{\mathrm{T}}(t)\left[\delta\boldsymbol{\omega}_k^{\times}(t) + \boldsymbol{R}_k(t)\boldsymbol{\omega}_d(t)\right]^{\times}\boldsymbol{J}\boldsymbol{\omega}_k(t)\\ =&\,\delta\boldsymbol{\omega}_k^{\mathrm{T}}(t)\left[\boldsymbol{R}_k(t)\boldsymbol{\omega}_d(t)\right]^{\times}\boldsymbol{J}\boldsymbol{\omega}_k(t)\end{aligned}$$

$$= \delta\boldsymbol{\omega}_k^{\mathrm{T}}(t)\left[\boldsymbol{R}_k(t)\boldsymbol{\omega}_d(t)\right]^{\times}\boldsymbol{J}\delta\boldsymbol{\omega}_k(t) + \delta\boldsymbol{\omega}_k^{\mathrm{T}}(t)\left[\boldsymbol{R}_k(t)\boldsymbol{\omega}_d(t)\right]^{\times}\boldsymbol{J}\boldsymbol{R}_k(t)\boldsymbol{\omega}_d(t), \tag{24}$$

where (3) is applied in (24) according to the property of the vector cross-product operator. To proceed, we have

$$\begin{aligned}\dot{V}_{\omega,k}(t) \le &-\delta\boldsymbol{\omega}_k^{\mathrm{T}}(t)\boldsymbol{J}\left[\boldsymbol{R}_k(t)\boldsymbol{\omega}_d(t)\right]^{\times}\delta\boldsymbol{\omega}_k(t)\\ &-\delta\boldsymbol{\omega}_k^{\mathrm{T}}(t)\left[\boldsymbol{R}_k(t)\boldsymbol{\omega}_d(t)\right]^{\times}\boldsymbol{J}\delta\boldsymbol{\omega}_k(t)\\ &-\delta\boldsymbol{\omega}_k^{\mathrm{T}}(t)\left[\boldsymbol{R}_k(t)\boldsymbol{\omega}_d(t)\right]^{\times}\boldsymbol{J}\boldsymbol{R}_k(t)\boldsymbol{\omega}_d(t)\\ &-\delta\boldsymbol{\omega}_k^{\mathrm{T}}(t)\boldsymbol{J}\boldsymbol{R}_k(t)\dot{\boldsymbol{\omega}}_d(t)+\beta_d(t)\left\|\delta\boldsymbol{\omega}_k^{\mathrm{T}}(t)\right\|\\ &+\delta\boldsymbol{\omega}_k^{\mathrm{T}}(t)\boldsymbol{u}_k(t)\end{aligned} \tag{25}$$

by combining (23) and (24) into (22) and utilizing the fact $\delta\boldsymbol{\omega}_k^{\mathrm{T}}(t)\boldsymbol{d}_k(t) \le \beta_d(t)\left\|\delta\boldsymbol{\omega}_k^{\mathrm{T}}(t)\right\|$. Furthermore, it is not difficult to obtain

$$\delta\boldsymbol{\omega}_k^{\mathrm{T}}(t)\left[\boldsymbol{R}_k(t)\boldsymbol{\omega}_d(t)\right]^{\times}\boldsymbol{J}\delta\boldsymbol{\omega}_k(t) + \delta\boldsymbol{\omega}_k^{\mathrm{T}}(t)\boldsymbol{J}\left[\boldsymbol{R}_k(t)\boldsymbol{\omega}_d(t)\right]^{\times}\delta\boldsymbol{\omega}_k(t) = 0, \tag{26}$$

$$\left\|\left[\boldsymbol{R}_k(t)\boldsymbol{\omega}_d(t)\right]^{\times}\right\| = \left\|\boldsymbol{R}_k(t)\boldsymbol{\omega}_d(t)\right\| = \left\|\boldsymbol{\omega}_d(t)\right\|, \tag{27}$$

$$\left\|\boldsymbol{R}_k(t)\dot{\boldsymbol{\omega}}_d(t)\right\| = \left\|\dot{\boldsymbol{\omega}}_d(t)\right\| \tag{28}$$

according to Lemma 1. Hence, substituting (26)–(28) into (25) leads to

$$\begin{aligned}\dot{V}_{\omega,k}(t) \le &-\delta\boldsymbol{\omega}_k^{\mathrm{T}}(t)\left[\boldsymbol{R}_k(t)\boldsymbol{\omega}_d(t)\right]^{\times}\boldsymbol{J}\boldsymbol{R}_k(t)\boldsymbol{\omega}_d(t)+\delta\boldsymbol{\omega}_k^{\mathrm{T}}(t)\boldsymbol{u}_k(t)\\ &-\delta\boldsymbol{\omega}_k^{\mathrm{T}}(t)\boldsymbol{J}\boldsymbol{R}_k(t)\dot{\boldsymbol{\omega}}_d(t)+\beta_d(t)\left\|\delta\boldsymbol{\omega}_k^{\mathrm{T}}(t)\right\|\\ \le&\left[\|\boldsymbol{J}\|\,\|\boldsymbol{\omega}_d(t)\|^2+\|\boldsymbol{J}\|\,\|\dot{\boldsymbol{\omega}}_d(t)\|+\beta_d(t)\right]\left\|\delta\boldsymbol{\omega}_k^{\mathrm{T}}(t)\right\|\\ &+\delta\boldsymbol{\omega}_k^{\mathrm{T}}(t)\boldsymbol{u}_k(t).\end{aligned} \tag{29}$$

Take the sum of (20) and (29), we have

$$\begin{aligned}&\dot{V}_{q,k}(t)+\dot{V}_{\omega,k}(t)\\ &\le\left[\|\boldsymbol{J}\|+\|\boldsymbol{J}\|\,\|\boldsymbol{\omega}_d(t)\|^2+\|\boldsymbol{J}\|\,\|\dot{\boldsymbol{\omega}}_d(t)\|+\beta_d(t)\right]\left\|\delta\boldsymbol{\omega}_k^{\mathrm{T}}(t)\right\|\\ &\quad+\delta\boldsymbol{\omega}_k^{\mathrm{T}}(t)\boldsymbol{u}_k(t)\\ &\le\theta(t)\left\|\delta\boldsymbol{\omega}_k^{\mathrm{T}}(t)\right\|+\delta\boldsymbol{\omega}_k^{\mathrm{T}}(t)\boldsymbol{u}_k(t)\\ &\le\theta(t)\left\|\delta\boldsymbol{\omega}_k^{\mathrm{T}}(t)\right\|_\infty+\delta\boldsymbol{\omega}_k^{\mathrm{T}}(t)\boldsymbol{u}_k(t)\\ &=\theta(t)\delta\boldsymbol{\omega}_k^{\mathrm{T}}(t)\,\mathrm{sgn}\,(\delta\boldsymbol{\omega}_k(t))+\delta\boldsymbol{\omega}_k^{\mathrm{T}}(t)\boldsymbol{u}_k(t),\end{aligned} \tag{30}$$

where (9) is applied and the definitions of the norms in *Notations* are considered.

Since $0 \le \zeta_k(t) < 1$, by substituting (30) into (19) and considering (8), we have

$$\begin{aligned}\dot{V}_k(t) &\le \zeta_k(t)\left[\theta(t)\delta\boldsymbol{\omega}_k^{\mathrm{T}}(t)\,\mathrm{sgn}\,(\delta\boldsymbol{\omega}_k(t))+\delta\boldsymbol{\omega}_k^{\mathrm{T}}(t)\boldsymbol{u}_k(t)\right]\\ &=\zeta_k(t)\tilde{\theta}_k(t)\delta\boldsymbol{\omega}_k^{\mathrm{T}}(t)\,\mathrm{sgn}\,(\delta\boldsymbol{\omega}_k(t))-\zeta_k(t)\delta\boldsymbol{\omega}_k^{\mathrm{T}}(t)\boldsymbol{K}_d\delta\boldsymbol{\omega}_k(t).\end{aligned} \tag{31}$$

By substituting (31) into (18), we can obtain

$$\begin{aligned}\Delta W_k(t) \le &-\frac{1}{2}\int_0^t\left[2\gamma^{-1}\bar{\theta}_k(\tau)\tilde{\theta}_k(\tau)+\gamma^{-1}\bar{\theta}_k^2(\tau)\right]\mathrm{d}\tau\\ &+\int_0^t\zeta_k(\tau)\tilde{\theta}_k(\tau)\delta\boldsymbol{\omega}_k^{\mathrm{T}}(\tau)\,\mathrm{sgn}\,(\delta\boldsymbol{\omega}_k(\tau))\,\mathrm{d}\tau\\ &-\int_0^t\zeta_k(\tau)\delta\boldsymbol{\omega}_k^{\mathrm{T}}(\tau)\boldsymbol{K}_d\delta\boldsymbol{\omega}_k(\tau)\mathrm{d}\tau-V_{k-1}(t)\\ =&-V_{k-1}(t)-\int_0^t\zeta_k(\tau)\delta\boldsymbol{\omega}_k^{\mathrm{T}}(\tau)\boldsymbol{K}_d\delta\boldsymbol{\omega}_k(\tau)\mathrm{d}\tau\\ &-\frac{1}{2\gamma}\int_0^t\bar{\theta}_k^2(\tau)\mathrm{d}\tau\\ \le&\ 0,\end{aligned} \tag{32}$$

where the parametric updating law (10) is utilized.

Part (2): The boundedness of $W_0(t)$**.** According to (13) and (31), the derivative of $W_0(t)$ can be calculated as

$$\begin{aligned}\dot{W}_0(t) &= \dot{V}_0(t)+\frac{1}{2}\gamma^{-1}\tilde{\theta}_0^2(t)\\ &\le\zeta_0(t)\delta\boldsymbol{\omega}_0^{\mathrm{T}}(t)\left[\tilde{\theta}_0(t)\,\mathrm{sgn}\,(\delta\boldsymbol{\omega}_0(t))-\boldsymbol{K}_d\delta\boldsymbol{\omega}_0(t)\right]\\ &\quad+\frac{1}{2}\gamma^{-1}\tilde{\theta}_0^2(t)\\ &=\left[\gamma\zeta_0(t)\delta\boldsymbol{\omega}_0^{\mathrm{T}}(t)\,\mathrm{sgn}\,(\delta\boldsymbol{\omega}_0(t))+\frac{1}{2}\tilde{\theta}_0(t)\right]\gamma^{-1}\tilde{\theta}_0(t)\\ &\quad-\zeta_0(t)\delta\boldsymbol{\omega}_0^{\mathrm{T}}(t)\boldsymbol{K}_d\delta\boldsymbol{\omega}_0(t)\\ &\le\left[\gamma\zeta_0(t)\delta\boldsymbol{\omega}_0^{\mathrm{T}}(t)\,\mathrm{sgn}\,(\delta\boldsymbol{\omega}_0(t))+\frac{1}{2}\tilde{\theta}_0(t)\right]\gamma^{-1}\tilde{\theta}_0(t).\end{aligned} \tag{33}$$

As $\hat{\theta}_{-1}(t) = 0$ for all $t \in [0, T]$, it is obvious that $\hat{\theta}_0(t) = \theta(t) - \tilde{\theta}_0(t) = \gamma\zeta_0(t)\delta\boldsymbol{\omega}_0^{\mathrm{T}}(t)\,\mathrm{sgn}\,(\delta\boldsymbol{\omega}_0(t))$, which gives

$$\begin{aligned}\dot{W}_0(t) &\le\left[\hat{\theta}_0(t)+\frac{1}{2}\tilde{\theta}_0(t)\right]\gamma^{-1}\tilde{\theta}_0(t)\\ &=\gamma^{-1}\theta(t)\tilde{\theta}_0(t)-\frac{1}{2}\gamma^{-1}\tilde{\theta}_0^2(t).\end{aligned} \tag{34}$$

By Young inequality, there exists a constant k_1 satisfying $0 < k_1 \le \frac{1}{2}\gamma$ such that

$$\gamma^{-1}\theta(t)\tilde{\theta}_0(t) \le k_1\gamma^{-2}\tilde{\theta}_0^2(t)+\frac{1}{4k_1}\theta^2(t). \tag{35}$$

Hence, by substituting (35) into (34), we have

$$\dot{W}_0(t) \le \frac{1}{4k_1}\theta^2(t). \tag{36}$$

Therefore, the boundedness of $\dot{W}_0(t)$ can be implied by the boundedness of $\theta(t)$, which thus leads to the uniform boundedness of $W_0(t)$ over $[0, T]$. In addition, due to the non-increasing property of $W_k(t)$ along the iteration axis, we can derive that $W_k(t)$ is uniformly bounded for $t \in [0, T]$ and $k \in \mathbb{Z}_+$, which implies the boundedness of the tracking errors $\delta\boldsymbol{q}_k(t)$, $\delta\boldsymbol{\omega}_k(t)$, the estimation error $\tilde{\theta}_k(t)$ and the control input $\boldsymbol{u}_k(t)$.

Part (3): The convergence of the tracking errors $\delta\boldsymbol{\omega}_k(t)$ **and** $\delta\boldsymbol{q}_k(t)$**.** For $\forall k \in \mathbb{Z}_+\backslash\{0\}$, we have the following inequality:

$$W_k(t) = W_0(t)+\sum_{j=1}^{k}\Delta W_j(t) \le W_0(t)-\sum_{j=1}^{k}V_{j-1}(t),$$

where the inequality (32) is used.

Due to the boundedness of $W_0(t)$ and the positiveness of $W_k(t)$, we can obtain that $\sum_{j=1}^{k}V_{j-1}(t)$ is convergent, which gives $\lim_{k\to\infty}V_k(t) = 0$ for $t \in [0, T]$ and thus leads to

$$\limsup_{k\to\infty}E_k(t) \le \beta_{dz} \quad \forall t \in [0, T]. \tag{37}$$

Therefore, the following results can be obtained:

$$\begin{cases}\limsup_{k\to\infty}\|\delta\boldsymbol{q}_k(t)\| \le \beta_{\delta q_{\sup}}\\ \limsup_{k\to\infty}\|\delta\boldsymbol{\omega}_k(t)\| \le \beta_{\delta\omega_{\sup}}\end{cases} \quad \forall t \in [0, T], \tag{38}$$

where $\beta_{\delta q_{\sup}} = \beta_{\delta\omega_{\sup}} = \left[2k_J\lambda_{\min}^{-1}(\boldsymbol{J})\lambda_{\max}(\boldsymbol{J}_n)\right]^{\frac{1}{2}}\left(\beta_{\delta q0}^2+\beta_{\delta\omega0}^2\right)^{\frac{1}{2}}$.

Remark 6. From Theorem 5, it is worthwhile to mention that by virtue of the newly designed parametric updating law equipped with a deadzone mechanism, the proposed adaptive ILC scheme is capable of dealing with more generic nonlinear systems with the unmodeled dynamics, iteration-varying disturbances as well as initial alignment errors. Additionally, thanks to the quaternion-based description of the system model, various system uncertainties can be treated together by a single scalar parametric updating law, which would reduce the estimation complexity

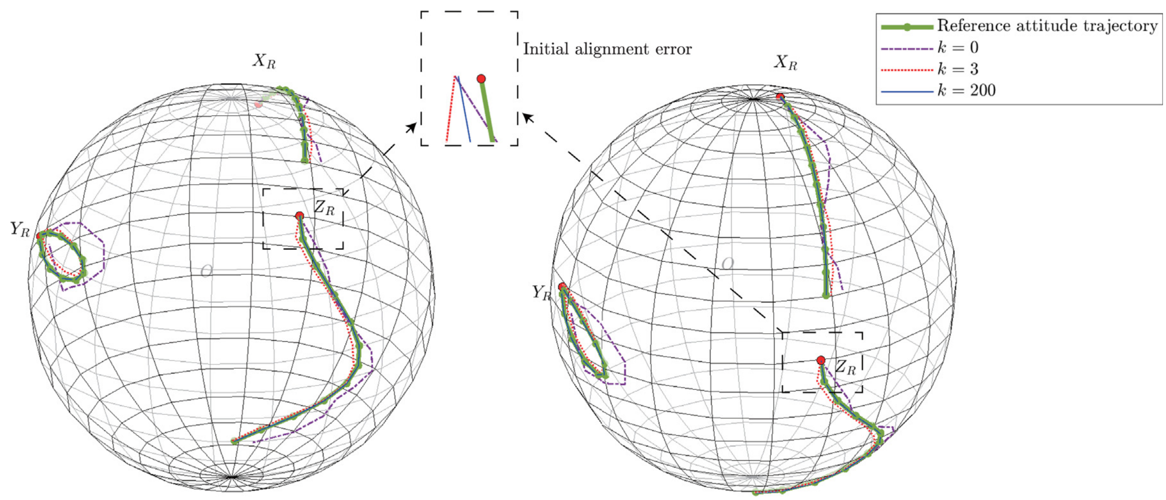

Fig. 2. Attitude tracking trajectories on attitude sphere from almost identical initial attitude. Red dot: the starting point of the reference trajectory. Left: view the trajectory using an azimuth of −60 deg and an elevation of −22 deg. Right: view the trajectory using an azimuth of −60 deg and an elevation of 22 deg.

of system uncertainties. Overall, in contrast to existing works, e.g., Jin (2017), Tayebi (2004), Wu et al. (2015), the present work does not only make the adaptive ILC method applicable to more practical systems, but also provide a new design and analysis framework for adaptive ILC of nonlinear systems operating in nonrepeatable environments.

As a special case, when $\beta_{\delta q0} = \beta_{\delta\omega 0} = 0$ holds, that is, i.i.c. is guaranteed, the perfect tracking performance can be achieved, and the result is summarized in the following Corollary 7, which is an immediate consequence from Theorem 5.

Corollary 7. *Consider the system (5) with i.i.c. (namely, $\beta_{dz} = 0$), and let the adaptive learning controller (8) and the parametric updating law (10) be applied. Then the perfect tracking objective (6) can be realized.*

Remark 8. In practice, the discontinuous control signals generated by (8) should be avoided since it might cause chattering that aggravates the effect of high-frequency unmodeled dynamics, and thus degrade the control performance. Smooth approximations of the sign operator in the controller (8), e.g., a hyperbolic tangent function, can be considered in practical applications by utilizing the techniques presented in Theorem 2 of Li et al. (2016).

5. A case study

In this section, to verify our results, we apply the proposed adaptive ILC scheme to the attitude tracking of rigid spacecraft with a Sun-synchronous orbit, which enables spacecraft to periodically observe the interested area on the Earth for some significant missions, such as reconnaissance, sensing, and imaging (Wu et al., 2015). When the interested area does not coincide with the ground track, the spacecraft is required to follow the identical attitude tracking trajectory perfectly over a fixed duration.

5.1. Simulation parameters

Before performing the simulations, we first describe the simulation parameters. In the present work, one spacecraft is required to periodically perform the attitude tracking task, where its orbit elements are given as follows: semimajor axis is 6778.20 km, eccentricity is 0, inclination is 97.64 deg, right ascension of the ascending node is 50.00 deg, argument of periapsis is 0, and true anomaly is 0. In order to detect the interested area on the earth by using the spacecraft, the initial value of reference quaternion and reference angular velocity $\boldsymbol{\omega}_d(t)$ are set as $\varepsilon_d(0) = 0.66$, $\boldsymbol{q}_d(0) = [0.34, -0.62, 0.25]^{\mathrm{T}}$, and

$$\boldsymbol{\omega}_d(t) = \begin{bmatrix} \frac{\pi}{12} \cdot \frac{\pi}{600} \sin(\frac{\pi}{600} t) \\ -\omega' \cos(-\frac{\pi}{12} \cos(\frac{\pi}{600} t) + \frac{\pi}{12}) \\ \omega' \sin(-\frac{\pi}{12} \cos(\frac{\pi}{600} t) + \frac{\pi}{12}) \end{bmatrix} \text{ rad/s},$$

respectively with the mean motion $\omega' = 0.0011$ rad/s, which is the required angular speed of the spacecraft to complete the orbit. In addition, T is set as 1200 s.

The nominal inertia matrix of the spacecraft in kg m^2 is given by $\boldsymbol{J}_n = \mathrm{diag}\,(20, 15, 15)$ and without loss of generality, $k_J = 0.8$ is considered. Moreover, initial alignment errors are arbitrary and bounded by $\beta_{\delta q0} = 0.001$ and $\beta_{\delta\omega 0} = 0.001$ rad/s.

In addition, the spacecraft is considered to suffer from the sine-wave disturbances in three axes (i.e., OX_B, OY_B, and OZ_B) with periods 40, 50, 70 s, and magnitudes of 0.1, 0.05, 0.08 Nm, respectively, and the initial phase of the disturbances to each axis is random. Note that the periodicity is not necessary and is just a special case.

For the proposed adaptive ILC scheme (8) and (10), the feedback gain $\boldsymbol{K}_d$ is set as $4\boldsymbol{I}_3$, and the parametric learning gain is chosen as $\gamma = 5$. It is worth noticing that $\boldsymbol{K}_d$ is closely related to the sampling time and can be roughly estimated by utilizing the method in Wie et al. (1989).

5.2. Simulation results

With the parameter settings mentioned above, the simulation results are presented in Figs. 2–4. In Fig. 2, the attitude trajectories of the spacecraft at different iterations are presented from different standpoints. After one iteration, the attitude of the rigid body will be reset to the small neighborhood of the desired initial attitude which is represented as the red starting dot. It is obvious that the tracking performance can be improved gradually via the proposed adaptive ILC scheme from iteration to iteration despite the presence of initial alignment errors. The convergence of the maximal attitude tracking error is illustrated in Fig. 3, where the error Euler angle defined as $\alpha_k(t) = 2\arccos([1 - \delta\boldsymbol{q}_k^{\mathrm{T}}(t)\delta\boldsymbol{q}_k(t)]^{\frac{1}{2}})$ is used to show the evolution of the attitude tracking error. We can see from Fig. 3 that the attitude tracking errors are uniformly bounded and enter a small neighborhood of the origin within a

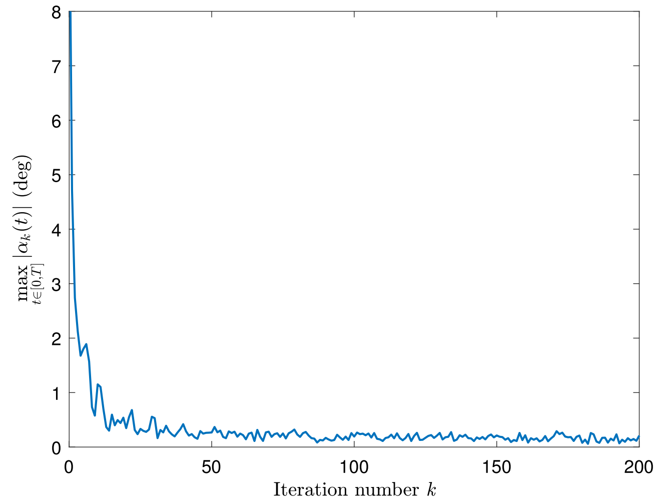

Fig. 3. $\max_{t\in[0,T]} |\alpha_k(t)|$ versus the number of iterations.

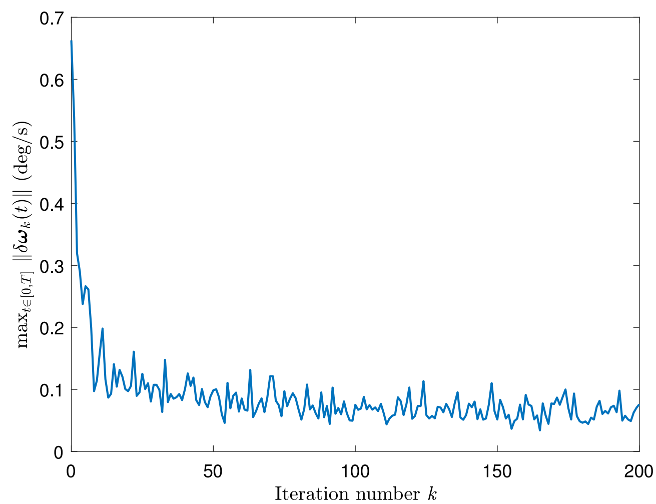

Fig. 4. $\max_{t\in[0,T]} \|\delta\boldsymbol{\omega}_k(t)\|$ versus the number of iterations.

finite number of iterations, despite unknown system parameters, external disturbances, and initial alignment errors. Additionally, the simulation results in terms of the angular velocity are shown in Fig. 4, where the convergence and uniform boundedness of the angular velocity error $\delta\boldsymbol{\omega}_k(t)$ are presented.

6. Conclusions

In the present work, a new design and analysis framework of adaptive ILC has been proposed for attitude tracking control of rigid bodies subject to uncertain nonlinear dynamics. In order to handle iteration-varying initial alignment errors, an adaptive ILC scheme together with a parametric updating law equipped with a deadzone mechanism has been developed, which is effective in avoiding the accumulation of initial alignment errors and thus ensuring the convergence of the proposed adaptive ILC scheme. Moreover, we have also shown that the proposed adaptive ILC scheme is capable of nullifying both the system uncertainties and external disturbances. The convergence of the adaptive ILC scheme has been analyzed under the framework of a Lyapunov-like theory by introducing a modified CEF, and finally, a practical example on attitude tracking of rigid spacecraft has been provided, which has verified the robust and high-precision performance of the proposed adaptive ILC scheme.

Acknowledgment

The authors would like to thank Dr. J. Zhang from Beihang University for his helpful discussions and suggestions.

Appendix. Proof of Lemma 1

Proof. According to the property of the vector cross-product operator, the following equation is obvious:

$$\begin{aligned}&\left[\delta\varepsilon_k(t)\boldsymbol{I}_3 - \delta\boldsymbol{q}_k^{\times}(t)\right]^{\mathrm{T}}\left[\delta\varepsilon_k(t)\boldsymbol{I}_3 - \delta\boldsymbol{q}_k^{\times}(t)\right]\\ &= \left[\delta\varepsilon_k(t)\right]^2\boldsymbol{I}_3 - \delta\boldsymbol{q}_k^{\times}(t)\delta\boldsymbol{q}_k^{\times}(t).\end{aligned}$$

And it can be obtained that the eigenvalues of $\delta\boldsymbol{q}_k^{\times}(t)\delta\boldsymbol{q}_k^{\times}(t)$ are $[\delta\varepsilon_k(t)]^2 - 1$, $[\delta\varepsilon_k(t)]^2 - 1$, and 0. Considering the definition of $\delta\varepsilon_k(t)$ in (2), we have $0 \le [\delta\varepsilon_k(t)]^2 \le 1$ accordingly. Thus, the following equation $\left\|\delta\varepsilon_k(t)\boldsymbol{I}_3 - \delta\boldsymbol{q}_k^{\times}(t)\right\| = 1$ always hold. Moreover, from the expression of the quaternion and (2), we can obtain that $\left\|\delta\boldsymbol{q}_k(t)\right\| \le 1$. Statement (2) follows from (4) because of the definition of the quaternion. Statement (3) can be verified easily from the information that $\boldsymbol{J}$ is symmetric.

References

Ahmed, J., Coppola, V. T., & Bernstein, D. S. (1998). Adaptive asymptotic tracking of spacecraft attitude motion with inertia matrix identification. *Journal of Guidance, Control, and Dynamics*, *21*(5), 684–691.

Ahn, H. S., Chen, Y., & Moore, K. L. (2007). Iterative learning control: Brief survey and categorization. *IEEE Transactions on Systems, Man, and Cybernetics, Part C (Applications and Reviews)*, *37*(6), 1099–1121.

Bristow, D. A., Tharayil, M., & Alleyne, A. G. (2006). A survey of iterative learning control: A learning-based method for high-performance tracking control. *IEEE Control Systems Magazine*, *26*(3), 96–114.

Chaturvedi, N. A., Sanyal, A. K., & McClamroch, N. H. (2011). Rigid-body attitude control. *IEEE Control Systems Magazine*, *31*(3), 30–51.

Chen, Y., Meng, T., Wang, Y., Wang, K., Meng, S., & Huang, D. (2019). Iterative learning control of two-phase laminar flow interface in Y-shaped microfluidic channel. *IEEE Transactions on Control Systems Technology*, *27*(6), 2743–2748.

Chien, C.-J. (2008). A combined adaptive law for fuzzy iterative learning control of nonlinear systems with varying control tasks. *IEEE Transactions on Fuzzy Systems*, *16*(1), 40–51.

Chien, C. J., & Tayebi, A. (2008). Further results on adaptive iterative learning control of robot manipulators. *Automatica*, *44*(3), 830–837.

Chou, J. C. K. (1992). Quaternion kinematic and dynamic differential equations. *IEEE Transactions on Robotics and Automation*, *8*(1), 53–64.

Dai, X., Quan, Q., Ren, J., & Cai, K. (2018). Iterative learning control and initial value estimation for probe-drogue autonomous aerial refueling of UAVs. *Aerospace Science and Technology*, *82–83*, 583–593.

French, M., & Rogers, E. (2000). Non-linear iterative learning by an adaptive Lyapunov technique. *International Journal of Control*, *73*(10), 840–850.

He, W., Meng, T., He, X., & Sun, C. (2019). Iterative learning control for a flapping wing micro aerial vehicle under distributed disturbances. *IEEE Transactions on Cybernetics*, *49*(4), 1524–1535.

He, W., Meng, T., Huang, D., & Li, X. (2018). Adaptive boundary iterative learning control for an Euler–Bernoulli beam system with input constraint. *IEEE Transactions on Neural Networks and Learning Systems*, *29*(5), 1539–1549.

Hu, Q., Xiao, B., Wang, D., & Poh, E. K. (2013). Attitude control of spacecraft with actuator uncertainty. *Journal of Guidance, Control, and Dynamics*, *36*(6), 1771–1776.

Hughes, P. C. (2004). *Spacecraft attitude dynamics*. Mineola, New York: Dover Publications.

Jin, X. (2017). Iterative learning control for non-repetitive trajectory tracking of robot manipulators with joint position constraints and actuator faults. *International Journal of Adaptive Control and Signal Processing*, *31*(6), 859–875.

Lee, J. H., & Lee, K. S. (2007). Iterative learning control applied to batch processes: An overview. *Control Engineering Practice*, *15*(10), 1306–1318.

Li, X., Huang, D., Chu, B., & Xu, J.-X. (2016). Robust iterative learning control for systems with norm-bounded uncertainties. *International Journal of Robust and Nonlinear Control*, *26*(4), 697–718.

Luo, W., Chu, Y.-C., & Ling, K.-V. (2005). Inverse optimal adaptive control for attitude tracking of spacecraft. *IEEE Transactions on Automatic Control*, *50*(11), 1639–1654.

Meng, D. (2019). Convergence conditions for solving robust iterative learning control problems under nonrepetitive model uncertainties. *IEEE Transactions on Neural Networks and Learning Systems*, *30*(6), 1908–1919.
Meng, D., & Moore, K. L. (2017). Robust iterative learning control for non-repetitive uncertain systems. *IEEE Transactions on Automatic Control*, *62*(2), 907–913.
Meng, D., & Zhang, J. (2018). Deterministic convergence for learning control systems over iteration-dependent tracking intervals. *IEEE Transactions on Neural Networks and Learning Systems*, *29*(8), 3885–3892.
Sun, M., & Wang, D. (2002). Iterative learning control with initial rectifying action. *Automatica*, *38*(7), 1177–1182.
Sutyasadi, P., & Parnichun, M. (2015). Trotting control of a quadruped robot using PID-ILC. In *Proceedings of the 41st annual conference of the IEEE industrial electronics society* (pp. 004400–004405).
Tayebi, A. (2004). Adaptive iterative learning control for robot manipulators. *Automatica*, *40*(7), 1195–1203.
Wen, J. T., & Kreutz-Delgado, K. (1991). The attitude control problem. *IEEE Transactions on Automatic Control*, *36*(10), 1148–1162.
Wie, B., Weiss, H., & Arapostathis, A. (1989). Quaternion feedback regulator for spacecraft eigenaxis rotations. *Journal of Guidance, Control, and Dynamics*, *12*(3), 375–380.
Wu, B., Wang, D., & Poh, E. K. (2015). High precision satellite attitude tracking control via iterative learning control. *Journal of Guidance, Control, and Dynamics*, *38*(3), 528–534.
Xie, H., & Sun, M. (2009). Design of iterative learning controllers with finite-time dead-zone modification. *Control Theory & Applications*, *26*(11), 1225–1231.
Xu, J.-X. (2011). A survey on iterative learning control for nonlinear systems. *International Journal of Control*, *84*(7), 1275–1294.
Xu, J.-X., & Tan, Y. (2002). A composite energy function-based learning control approach for nonlinear systems with time-varying parametric uncertainties. *IEEE Transactions on Automatic Control*, *47*(11), 1940–1945.
Xu, J.-X., & Yan, R. (2005). On initial conditions in iterative learning control. *IEEE Transactions on Automatic Control*, *50*(9), 1349–1354.
Yu, M., & Li, C. (2017). Robust adaptive iterative learning control for discrete-time nonlinear systems with time-iteration-varying parameters. *IEEE Transactions on Systems, Man, and Cybernetics: Systems*, *47*(7), 1737–1745.
Yu, M., Wang, J., & Qi, D. (2013). Discrete-time adaptive iterative learning control for high-order nonlinear systems with unknown control directions. *International Journal of Control*, *86*(2), 299–308.
Zou, A., Kumar, K. D., & de Ruiter, A. H. J. (2020). Fixed-time attitude tracking control for rigid spacecraft. *Automatica*, *113*, Article 108792.

Fan Zhang received the B.Eng. degree in detection, guidance and control technology and the M.Eng. degree in navigation, guidance and control from the School of Astronautics, Northwestern Polytechnical University (NWPU), Xi'an, China, in 2015 and 2018, respectively. He is currently pursuing the Ph.D. degree with the School of Automation Science and Electrical Engineering, Beihang University (BUAA), Beijing, China. His current research interests include iterative learning control, networked control systems and space flight dynamics and control.

Deyuan Meng received the B.S. degree in mathematics and applied mathematics from Ocean University of China (OUC), Qingdao, China, in June 2005, and the Ph.D. degree in control theory and control engineering from Beihang University (BUAA), Beijing, China, in July 2010. From November 2012 to November 2013, he was a Visiting Scholar with the Department of Electrical Engineering and Computer Science, Colorado School of Mines, Golden, CO, USA. He is currently a Full Professor with the Seventh Research Division and the School of Automation Science and Electrical Engineering, Beihang University (BUAA). His current research interests include iterative learning control, data-driven control, and multi-agent systems.

Xuefang Li received the B.Sc. and M.Sc. degrees with a major of pure mathematics from the Mathematical College, Sichuan University, Chengdu, China, in 2009 and 2012, respectively. She attended the Department of Electrical and Computer Engineering (ECE), National University of Singapore (NUS), Singapore, in 2012, where she received the Ph.D. degree with a major in control engineering in 2016. From September 2016 to August 2019, she was a Research Associate with the Department of Electrical and Electronic Engineering (EEE), Imperial College London, London, U.K. She is currently an Associate Professor with the School of Intelligent Systems Engineering, Sun Yat-Sen University, Guangzhou, China. Her research interests include advanced control theory, robotics, and intelligent vehicles. She is a member of the IEEE CSS and IEEE IES.